Video Article

Fabrication of Fully Solution Processed Inorganic Nanocrystal Photovoltaic Devices

Troy K. Townsend[1], Dario Durastanti[1], William B. Heuer[2], Edward E. Foos[3], Woojun Yoon[4], Joseph G. Tischler[4]

[1]Department of Chemistry and Biochemistry, St. Mary's College of Maryland

[2]Department of Chemistry, U.S. Naval Academy

[3]NSWC Indian Head EOD Technology Division

[4]Electronics and Devices Division, Naval Research Laboratory

Correspondence to: Troy K. Townsend at tktownsend@smcm.edu

URL: http://www.jove.com/video/54154
DOI: doi:10.3791/54154

Keywords: Engineering, Issue 113, inorganic nanocrystals, nanomaterials, electronic inks, photovoltaics, solution process, synthesis, thin film devices, ligand exchange, spray coating, spin coating, transparent conductive film, physics

Date Published: 7/8/2016

Citation: Townsend, T.K., Durastanti, D., Heuer, W.B., Foos, E.E., Yoon, W., Tischler, J.G. Fabrication of Fully Solution Processed Inorganic Nanocrystal Photovoltaic Devices. *J. Vis. Exp.* (113), e54154, doi:10.3791/54154 (2016).

Abstract

We demonstrate a method for the preparation of fully solution processed inorganic solar cells from a spin and spray coating deposition of nanocrystal inks. For the photoactive absorber layer, colloidal CdTe and CdSe nanocrystals (3-5 nm) are synthesized using an inert hot injection technique and cleaned with precipitations to remove excess starting reagents. Similarly, gold nanocrystals (3-5 nm) are synthesized under ambient conditions and dissolved in organic solvents. In addition, precursor solutions for transparent conductive indium tin oxide (ITO) films are prepared from solutions of indium and tin salts paired with a reactive oxidizer. Layer-by-layer, these solutions are deposited onto a glass substrate following annealing (200-400 °C) to build the nanocrystal solar cell (glass/ITO/CdSe/CdTe/Au). Pre-annealing ligand exchange is required for CdSe and CdTe nanocrystals where films are dipped in NH_4Cl:methanol to replace long-chain native ligands with small inorganic Cl^- anions. $NH_4Cl_{(s)}$ was found to act as a catalyst for the sintering reaction (as a non-toxic alternative to the conventional $CdCl_{2(s)}$ treatment) leading to grain growth (136±39 nm) during heating. The thickness and roughness of the prepared films are characterized with SEM and optical profilometry. FTIR is used to determine the degree of ligand exchange prior to sintering, and XRD is used to verify the crystallinity and phase of each material. UV/Vis spectra show high visible light transmission through the ITO layer and a red shift in the absorbance of the cadmium chalcogenide nanocrystals after thermal annealing. Current-voltage curves of completed devices are measured under simulated one sun illumination. Small differences in deposition techniques and reagents employed during ligand exchange have been shown to have a profound influence on the device properties. Here, we examine the effects of chemical (sintering and ligand exchange agents) and physical treatments (solution concentration, spray-pressure, annealing time and annealing temperature) on photovoltaic device performance.

Video Link

The video component of this article can be found at http://www.jove.com/video/54154/

Introduction

Due to their unique emerging properties, inorganic nanocrystal inks have found applications in a wide range of electronic devices including photovoltaics,[1-6] light emitting diodes,[7,8] capacitors[9] and transistors.[10] This is due to the combination of the excellent electronic and optical properties of inorganic materials and their solution compatibility on the nanoscale. Bulk inorganic materials are typically not soluble and are therefore limited to high temperature, low pressure vacuum depositions. However, when prepared on the nanoscale with an organic ligand shell, these materials can be dispersed in organic solvents and deposited from solution (drop-, dip-, spin-, spray- coating). This freedom to coat large and irregular surfaces with electronic devices reduces the cost of these technologies while also expanding possible niche applications.[6,11,12]

Solution processing of cadmium(II) telluride (CdTe), cadmium(II) selenide (CdSe), cadmium(II) sulfide (CdS) and zinc oxide (ZnO) inorganic semiconductor active layers has led to photovoltaic devices reaching efficiencies (η) for metal-CdTe Schottky junction CdTe/Al (η = 5.15%)[13,14] and heterojunction CdS/CdTe (η = 5.73%),[15] CdSe/CdTe (η = 3.02%),[16,17] ZnO/CdTe (η = 7.1%, 12%).[18,19] In contrast to vacuum deposition of bulk CdTe devices, these nanocrystal films must undergo ligand exchange following deposition to remove native and insulating long-chain organic ligands which prohibit efficient electron transport through the film. Additionally, sintering Cd- (S, Se, Te) must occur during heating in the presence of a suitable salt catalyst. Recently, it was found that non-toxic ammonium chloride (NH_4Cl) can be used for this purpose as a replacement for the commonly used cadmium(II) chloride ($CdCl_2$).[20] By dipping the deposited nanocrystal film in NH_4Cl:methanol solutions, the ligand exchange reaction occurs simultaneously with exposure to the heat-activated NH_4Cl sintering catalyst. These prepared films are heated layer-by-layer to build the desired thickness of the photo-active layers.[21]

Recent advances in transparent conductive films (metal nanowires, graphene, carbon nanotubes, combustion processed indium tin oxide) and conductive metal nanocrystal inks have led to the fabrication of flexible or curved electronics built on arbitrary non-conductive surfaces.[22,23] In

this presentation, we demonstrate the preparation of each precursor ink solution including the active layers (CdTe and CdSe nanocrystals), the transparent conducting oxide electrode (*i.e.*, indium doped tin oxide, ITO) and the back metal contact to construct a completed inorganic solar cell entirely from a solution process.[24] Here, we highlight the spray process and the device layer patterning architectures on non-conductive glass. This detailed video protocol is intended to aid researchers who are designing and building solution processed solar cells; however, the same techniques described here are applicable to a wide range of electronic devices.

Protocol

Note: Please consult all relevant materials safety data sheets (MSDS) before use. Many of the precursor solutions and products are hazardous or carcinogenic. Special consideration should be directed to nanomaterials due to unique safety concerns that arise compared to their bulk counterparts. Proper protective equipment should be worn (safety goggles, face shield, gloves, lab coat, long pants and closed-toed shoes) at all times during this procedure.

1. Synthesis of Nanocrystal Precursor Inks

1. **CdSe and CdTe Inks**[18,25]
    1. In an inert atmosphere glove box, combine 0.24 g (0.0019 mol) tellurium (Te) for CdTe (or 0.1527 g (0.0019 mol) selenium (Se) for CdSe) powder with 4.39 g (0.012 mol) trioctylphosphine (TOP) into a 5 ml round bottom flask (RBF).
    2. Seal this flask with a rubber septum and remove from glove box for sonication (40 kHz) in a heated (60 °C) water bath until all of the solid Te or Se has dissolved (about 20 min). Set aside 5 ml of 1-octadecene (1-ODE).
    3. Separately, in a clean and dry 3-neck 250 ml RBF with a magnetic stir bar, combine 0.48 g (0.0037 mol) cadmium(II) oxide (CdO) powder with 4.29 g (0.015 mol) Oleic Acid (OA) and 76 ml of 1-octadecene. Inspect glassware for defects prior to use, and assemble all glass-to-glass joints with high temperature vacuum grease.
    4. Connect a vacuum pump and an inert gas (argon, Ar or nitrogen, N_2) source on low flow to the flask through a Schlenk line glassware leaving at least one neck of the RBF free to inject the TOP-chalcogenide precursor. Insert temperature probe directly into the solution from one of the necks and seal.
    5. Set to stir at the highest speed and set temperature to 110 °C under vacuum for 30 min.
    Note: Exceeding 250 °C may degrade the oleic acid component indicated by a color change from colorless to yellow.
    6. Switch from vacuum to inert gas to build a slight positive pressure in the flask. Adjust the flow of gas to a low pressure (~1 psi). Bubbles should be forming at a frequency of 1-5 Hz in the oil bubbler.
        1. Separately prepare a glass neck extension topped with a rubber septum. Attach a syringe needle to tubing on the Schlenk line.
        2. Pierce the syringe needle into the septum to allow pressure to release. Remember to lightly grease the joint with vacuum grease.
        3. At this time, quickly remove the top glass stopper from the reaction flask and replace it with a glass extension. Excess inert gas will flow through the flask, and this will be indicated with bubbles emerging from the oil bubbler.
    7. Close the original inert gas source and open the second vent to allow a slow controlled stream of inert gas into the top of the flask during the rest of the synthesis.
    8. Increase the temperature of the solution to 260 °C for CdTe (250 °C for CdSe) and wait until the solution turns from a slight brown to completely colorless and transparent.
    9. Once the desired reaction temperature is reached, prepare a syringe for injection by extracting the TOP-chalcogenide precursor and the additional 5 ml 1-ODE.
    10. In one step, remove the heating mantle while continuing to stir and rapidly inject the TOP-chalcogenide/1-ODE mixture.
    11. Allow solution to cool to RT (~30 min) and monitor color changes as quantum confined particle seeds form and grow into larger nanocrystals. CdSe is a deep red color and CdTe is a dark brown.
    12. Directly to the flask, add 25 ml heptane and 100 ml ethanol to precipitate the product. Transfer 40 ml aliquots to a 50 ml centrifuge tube and add 5 ml toluene and 5 ml ethanol to complete precipitation.
    13. Centrifuge the product at 1,722 x g for 2 min or until the supernatant is transparent. Decant supernatant and combine solid product into a 5 ml RBF by adding 0.5 ml toluene and 5 ml distilled pyridine to disperse the nanocrystals. CAUTION: Conduct all pyridine experiments under the fume hood.
    14. Flush the RBF with inert gas and then seal with rubber septum. Attach heating mantle and bring to 85 °C. Relieve any pressure using a needle inserted briefly into the rubber septum. Continue heating and stirring gently for 18 hr.
    15. Following pyridine exchange, combine CdTe or CdSe product and 40 ml hexanes and centrifuge at 1,722 x g for 2 min or until supernatant is colorless. Decant supernatant and add 5 ml distilled pyridine and 5 ml 1-propanol. Flush flask with inert gas and sonicate (40 kHz) this mixture for 30 min. Collect the supernatant and discard any solid product.
    16. Filter the ink through a 1 µm Polytetrafluoroethylene (PTFE) syringe filter to remove large or aggregated particles. Measure the concentration of the ink by drying and weighing 1 ml. Typical concentrations are 40 mg ml^{-1} for CdTe and 16 mg ml^{-1} for CdSe.
    17. Dilute ink with pyridine / 1-propanol as needed. Store ink under inert gas while not in use.

2. **Au Ink**[26]
    1. In a 500 ml Erlenmeyer flask while stirring, combine 1.518 g (0.00385 mol) of gold(III) chloride trihydrate, $HAuCl_4 \cdot 3H_2O$ and 126 ml H_2O to produce a yellow solution.
    2. Add a pre-mixed solution of 9.52 g (0.0174 mol) tetraoctylammonium bromide in 334 ml toluene.
    3. Next add the ligand, 0.452 g (0.00382 mol) hexanethiol in 2 ml toluene.
    4. Finally, separately combine 1.58 g (0.0418 mol) sodium borohydride ($NaBH_4$) with 105 ml H_2O and immediately add this bubbling reducing solution drop-wise to the reaction flask.
    5. After stirring at RT in air for 3 hr, separate the organic phase with a separatory funnel.
    6. Use a rotary evaporator to reduce the volume to 20 ml and wash this ink with 50 ml hexanes and 200 ml methanol. Precipitate solid with centrifugation at 1,722 x g for 2 min and decant the colorless supernatant.

7. Dry the solid in air and re-disperse in chloroform with a concentration of 70 mg ml^{-1}.

3. **ITO Inks**[23]
    1. Combine solid salts of indium(III) nitrate hydrate ($In(NO_3)_3 \cdot 2.85H_2O$, 2.93 g, 0.00974 mol) and tin(II) chloride dihydrate, ($SnCl_2 \cdot 2H_2O$, 0.357 g, 0.00158 mol) with 10 ml 2-methoxyethanol into a 50 ml polypropylene centrifuge tube.
    2. To this, add 167 µl of 14.5 M ammonium hydroxide (NH_4OH, 0.0024 mol) as a pH stabilizer and 0.83 g (0.0104 mol) ammonium nitrate (NH_4NO_3) as an oxidizer.
    3. Sonicate at 40 kHz for 20 min with heating (60 °C) or until the ink changes from hazy white to colorless and transparent.

2. ITO Patterning

1. Cut and clean a (25 mm x 25 mm x 1.1 mm) glass slide by sonicating in ethanol and acetone.
2. Soak glass substrate in concentrated (> 5 M) aqueous sodium hydroxide (NaOH) for 1 min and briefly rinse with water.
3. Place the glass substrate on the spin coater and fill slide with ITO ink. Spin at 3,228 x g for 20 sec.
4. Immediately place the substrate on a hotplate set to 400 °C and heat for 10 min. Cool slowly at RT on a ceramic plate.
5. Repeat this process (2.3 - 2.4) until the sheet resistance is below 1,000 Ohms per square (about 10 layers). Approximate the sheet resistance with a multimeter or measure with a four-point probe by placing the ITO/glass film on a stable surface and pressing down the multimeter probes approximately 0.5 cm apart to record the resistance. If a four-point probe is available, depress the probe tips onto the film to record the sheet resistance following established methods.[27]
6. Finally, briefly dip (~2 sec) the film in dilute aqua regia and rinse with distilled water followed by drying to reduce the resistance below 500 Ohms per square.
7. Construct a device pattern by cutting strips of tape (*i.e.*, polyamide tape for heat treatments or cellophane tape for acid etching) and adhering them along the pre-designed grid. For example, perpendicular strips with a width of 0.10 cm will produce 0.10 cm^2 device areas.
    1. Design grids with document editing software, print onto paper and position under the substrate to act as a guide for mounting tape onto the transparent glass slide.
    Note: Depending on the application and the properties of the inks, these grids can be used to produce devices with overlapping top and bottom electrodes in the shape of a square, a rectangle or any shape with measurable area. For example, by alternating two parallel strips of ITO that are each 0.10 cm wide, followed by depositing the active layers (CdSe and CdTe), the gold layer can be deposited using the same pattern only rotated by 90 degrees to form two 0.10 cm^2 devices.
8. Soak the glass/ITO film with adhered tape strips in dilute aqua regia at 60 °C until the exposed ITO dissolves, leaving behind bare glass substrate.
9. Remove the tape and wash film with acetone and ethanol to remove any residue from the tape adhesive.
10. Place small drops of silver epoxy on the ITO strips on one end of the glass substrate. Heat this on a hotplate at 150 °C for 2 min, followed by cooling to RT. These will serve as contact points for device measurement since it is difficult to remove the CdTe/CdSe active layers after annealing.

3. Solution Processing of CdSe, CdTe and Au Films

1. **Spin Coating**[28]
    1. Place patterned ITO-glass substrate on spin coater and fill the top surface by drop coating CdSe nanocrystals.
    2. Spin at 610 x g for 30 sec followed by drying on a hotplate at 150 °C for 2 min. Cool to 25 °C.
    3. Dip the film in a NH_4Cl:methanol (saturated at 25 °C) solution set to 60 °C. Hold for 15 sec and then dip film into a separate container of isopropanol.
    4. Dry under inert gas and then heat on a hotplate at 380 °C for 25 sec. Cool to RT and rinse off excess salt with distilled water before drying under inert gas.
    5. Repeat this process (3.1.1 - 3.1.4) until the desired thickness is reached. Typically, 3 layers of CdSe produce a 60 nm film and 6 layers of CdTe produces a 400 nm CdTe film.

2. **Spray Coating**[12,29]
    1. Mount the ITO-glass substrate vertically with tape or clips onto a flat solid backing.
    2. Dilute the CdTe and CdSe ink to 4 mg ml^{-1} with chloroform and load the gravity-fed airbrush (equipped with 0.5 mm needle) with 0.25 ml of the ink.
    3. Adjust the carrier gas pressure between 10 and 40 psi. Use higher pressures for thinner smoother films.
    4. Depress nozzle and spray nanocrystal ink next to the substrate followed by spraying uniformly over the substrate using a rapid perpendicular side-to-side motion where the air brush nozzle is kept approximately 60 mm from the substrate. Clean the airbrush by spraying ~1 ml pure chloroform away from the device.
    5. Remove substrate from the mount and treat the deposited CdTe or CdSe nanocrystal film with the same procedure as for spin coating (3.1.5) until the desired thickness is achieved.
    6. Likewise, spray the back metal contact nanocrystal film onto the active layers to complete the device. Using the same procedure employed for the ITO electrodes, pattern 0.01 cm thick strips using low-adhesive tape to the active layer perpendicular to the ITO strips.
    7. Load the airbrush with 2 ml of the gold (Au) nanocrystal ink (70 mg ml^{-1}) dispersed in chloroform.
    8. After a dark opaque film is deposited, dismount the substrate and carefully remove the tape before heating on a hotplate at 250 °C for 20 sec. The gold color will appear and the device can be cooled to RT and tested.

Representative Results

Small angle X-ray Diffraction Patterns are used to verify the crystallinity and phase of the annealed nanocrystal film (**Figure 1A**). If crystallite sizes are below 100 nm, their crystal diameter can be estimated with the Scherrer equation (Eq. 1) and verified with Scanning Electron Microscopy (SEM),

$$Eq.1 \quad d = \frac{K\lambda}{\beta cos\theta}$$

where d is the mean crystallite diameter, K is the dimensionless shape factor for the material, β is the full width half maximum of the X-ray Diffraction (XRD) peak at the Bragg angle θ.

Scanning Electron Microscopy (SEM) is used to monitor the extent of grain growth in the annealed films (**Figure 2B, C** and **Figure 3C-F**). After depositing a single layer of CdTe or CdSe and heating in the presence of NH_4Cl, grain size can be optimized by adjusting the temperature and duration of heating as well as the ink concentration, spray pressure/duration or spin speed. Typically, larger grains indicate devices with higher short circuit currents.[12] For profile images, the glass side of the device can be scored with a diamond scribe and cracked to produce a straight edge and mounted in the SEM vertically (**Figure 1B**).

UV/Vis Spectroscopy is used to estimate nanocrystal size based on absorbance peak correlation with quantum confinement effects (**Figure 1C-D**). Crystal size can be tuned by modifying the concentration of precursors, the reaction temperature and the duration of the ink synthesis.

Optical Profilometry is used to measure film thickness and roughness. This can be conducted on a single layer of each material and on completed devices (**Figure 3G-J**).

Fourier Transform Infrared (FTIR) Spectra are taken to monitor the degree of ligand exchange during the NH_4Cl:methanol treatment as measured by the disappearance of the C–H alkyl stretching bands at 2,924 and 2,852 cm^{-1} (**Figure 2A**).[20]

Current-Voltage (I-V) characteristics can be obtained in the dark and under simulated one sun illumination from a calibrated solar simulator (**Figure 2D, E**). Attaching the probe tips to the anode (Au) and the cathode (ITO), a photocurrent can be measured with a digital multimeter/ source meter. By scanning from negative to positive potential (Ex. -1.5 V to +1.5 V), an I-V curve is produced and provides data such as the open circuit voltage (V_{OC}) at 0.0 amps, the short circuit current (I_{SC}) at 0.0 volts, the fill factor (FF, Eq. 2) and the efficiency (η, Eq. 3),

$$Eq.2 \quad FF = \frac{J_{MP}\, V_{MP}}{J_{SC}\, V_{OC}}$$

where J_{MP} and V_{MP} are the current density and voltage at the maximum power point, respectively. If the software does not provide the FF, find the maximum power point by plotting the product of J and V as a function of V. For efficiency use,

$$Eq.3 \quad \eta = \frac{J_{SC}\, V_{OC}\, FF}{P_{in}}$$

where P_{in} is the power input per unit area from solar irradiance (100 mW/cm^2). By accounting for the device area (ex. 0.1 cm^2), the units cancel leaving a unitless fraction. Special consideration must be taken to mask the other devices on the substrate during measurement to avoid an excess photocurrent contribution from adjacent devices.

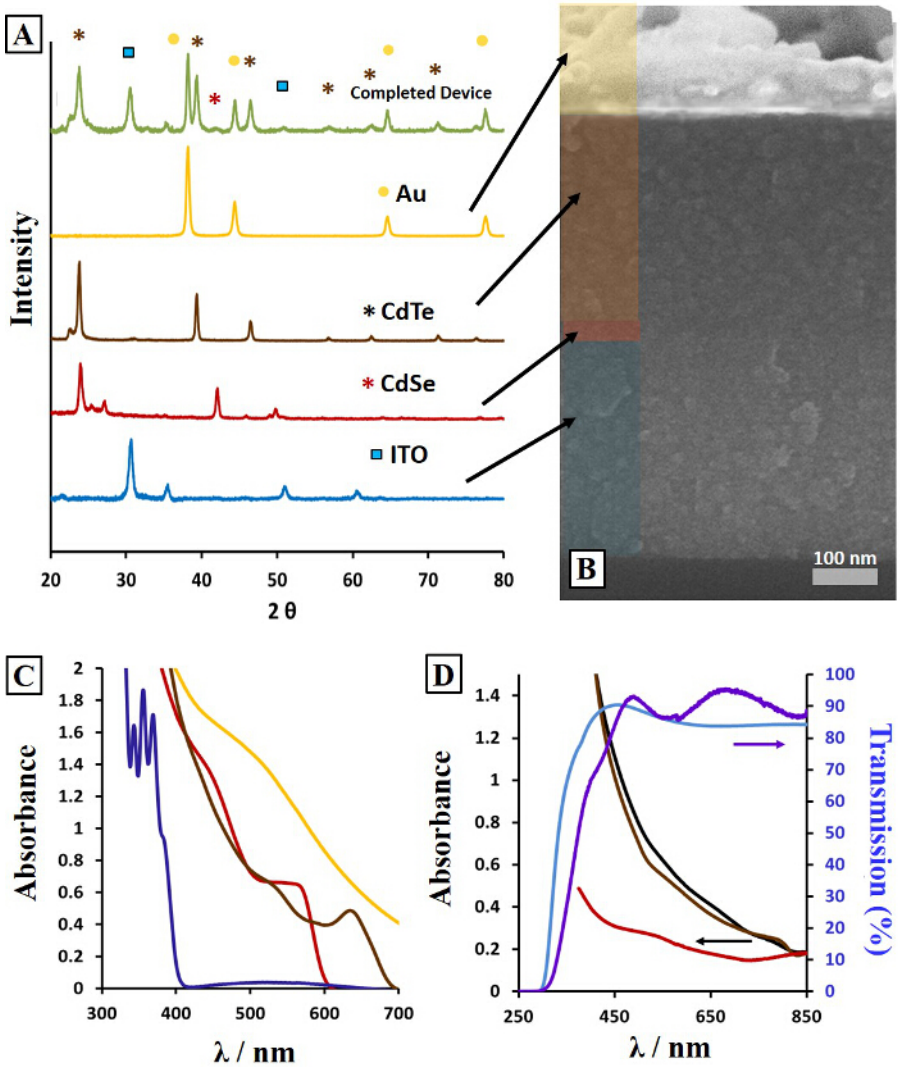

Figure 1. Film Characterization. X-ray diffraction patterns of each individual device layer as a single film and a completed device (**A**) including a cross-section SEM image of the device build from nanocrystal inks (**B**). UV/Vis spectra of commercial ITO (light blue) and ITO-sol (purple) on glass and absorption of CdSe-sol (red), CdTe-sol (brown) and CdSe-sol/CdTe-sol films together (black) on commercial ITO glass substrates (**D**), and absorption of nanocrystal precursor solutions of CdSe (red), CdTe (brown), Au (gold), and ITO (purple) prior to annealing (**C**). Adapted from Ref. 24 with permission from The Royal Society of Chemistry.[24] Please click here to view a larger version of this figure.

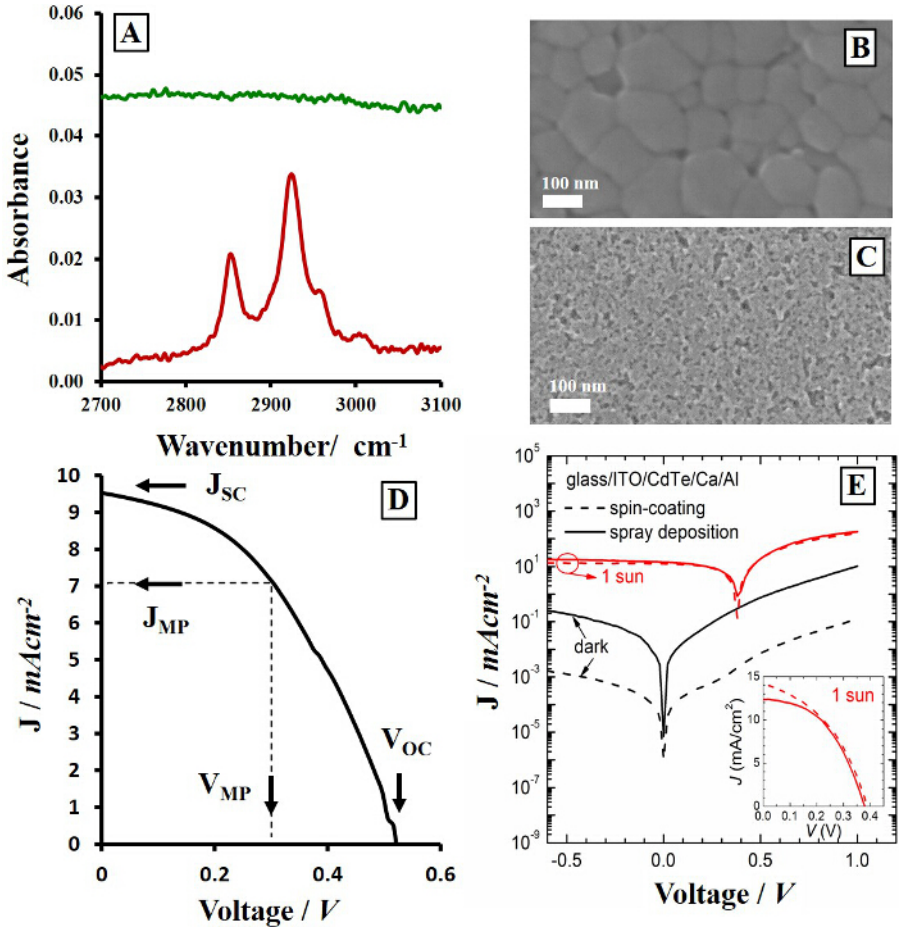

Figure 2. Ligand Exchange Catalyst and Device Properties. FTIR spectra of pyridine exchanged CdTe nanocrystal films (**A**) dipped in NH_4Cl:methanol solution (green) and in pure methanol (red) including corresponding SEM images of these films (**B** and **C**, respectively) after annealing at 380 °C for 25 sec. Current-voltage curves of an all solution processed CdSe/CdTe heterojunction device measured under 1 sun illumination (**D**) and a comparison of spin coated (---) and spray coated (-) Schottky devices (**E**) under 1 sun illumination (red) and in the dark (black). Reprinted with permission from Ref. 12. Copyright 2014 American Chemical Society and adapted from Ref. 20 and 24 with permission from The Royal Society of Chemistry.[20,24] Please click here to view a larger version of this figure.

The XRD patterns exhibit clear diffraction peaks at angles corresponding to the crystal lattice dimensions for each material and the completed device (**Figure 1A**). Scherrer size analysis estimates crystallite sizes on the order of 100 nm for CdTe films compared to the as-synthesized nanocrystals (3-5 nm). This transformation from quantum confined nanocrystals of CdSe and CdTe to red shifted bulk-scale grains in the annealed films is shown in the UV/Vis spectra of **Figure 1C-D**. The thickness of the deposited films can be increased by raising the concentration of the ink or increasing the number of layers for both spin coating and spray coating. The thickness and uniformity of the film is monitored by optical profilometry (**Figure 3B, G-J**). Spray coated films are typically rougher (51 ± 14 nm spray vs. 22 ± 12 nm spin), although this can be reduced with higher delivery pressures and less concentrated inks.[12] Once a target thickness and roughness is obtained on a single film on glass, the procedure can be applied to device fabrication. Cross-section images of the device display film thicknesses of each layer and verify intact interfaces between them (**Figure 1B**).[24]

As-synthesized nanocrystals contain a shell of long-chain native oleate ligands that interfere with film quality, leaving behind insolating organic material during heating. Pyridine exchange reactions were used to remove the oleate shell; however, as many have observed, this process is incomplete.[16,26,27] Following a 18 hr pyridine exchange, residual oleate ligands remain attached to the nanocrystals as observed by their characteristic infrared stretching frequencies of the C-H alkyl groups at 2,924 and 2,852 cm^{-1}. FTIR spectra in **Figure 2A** show the absence (green) and presence (red) of the native oleate ligand bound to the CdTe nanocrystals in the as-deposited pre-annealed film treated with the NH_4Cl:methanol ligand exchange catalyst and methanol only, respectively. This salt treatment simultaneously replaces the residual long-chain oleate ligands with small inorganic chloride anions, while aiding in the sintering reaction. In this situation, which is unique to nanocrystals, the ligand exchange agent must remove the native ligand while also providing excess adequate sintering catalyst on the surface. Both of these processes are key components of a successful CdTe device. Previous research demonstrated that the common usage of $CdCl_2$ can be replaced with non-toxic NH_4Cl for this purpose. The resulting average grain growth of 136 ± 39 nm after annealing is shown in **Figure 2B** for NH_4Cl treated CdTe films whereas no growth is observed for the methanol control (**Figure 2C**). Monitoring ligand exchange is a unique component of many nanocrystal electronic films compared to bulk scale vacuum deposition due to the inherent nature of bottom-up synthetic routes.[3,30] These involve the formation of organic ligand shells that provide solution solubility for the inorganic core, although this insulating shell does not typically contribute to the optoelectronic function of the film.

Solar cell devices measured under 1 sun illumination (**Figure 2D, E**) show current-voltage curves from 0.1 cm^2 devices. A characteristic device shown here produces V_{OC} = 0.52 ± 0.02 V, J_{SC} = 9.42 ± 3.2 mA cm^{-2}, FF (%) = 43.3 ± 2.9 and η (%) = 2.37 ± 0.23 under simulated sunlight.

However, due to the strong link between grain growth and processing methods, small changes in annealing temperature and heating time of CdTe films can lead to large variation in the open circuit voltages and short circuit currents of these nanocrystal films leading to reported Jsc values ranging from 0.7 mA/cm^2 to 25 mA/cm^2 and efficiencies above 10%.[12,31] Higher efficiencies are expected following enhancement of the quality and combination of materials for solution processed photovoltaics as well as other electronic devices and functional surfaces.

Compared to traditional spin-coating of nanocrystal films, spray-coating requires additional considerations due to the inherent freedoms of using an airbrush with adjustable delivery pressure, distance from substrate, angle of spray and duration. When maintaining constant CdTe ink concentrations (4 mg/ml) and nozzle distance to substrate (60 mm), increasing pressures were found to systematically decrease film roughness producing smoother, higher quality layers. **Figure 3** summarizes the effect of adjusting spray pressure on the film morphology and optical properties. As a result of increasing pressure from 15 psi to 40 psi, CdTe nanocrystal films showed higher optical transmittance (**Figure 3A**) as a result of being physically thinner (30 nm vs 95 nm per layer, **Figure 3B**). At higher pressures, the spray material is dispersed into a larger area around the target substrate and less material is deposited on the device. After annealing at 380 °C, the film of nanocrystals condense with a higher packing density as ligand molecules are released and the surface areas of individual nanocrystals are reduced to larger consolidated crystal grains. Therefore, thinner films of as-deposited nanocrystals undergo a smaller change in volume, leading to fewer cracks that appear after heating. This effect produces smoother films that are virtually identical to those deposited via spin-coating. This can be observed in the SEM images and corresponding optical profilometry maps (**Figure 3C-J**). After optimization of the spray parameters to achieve the desired film qualities, devices can be fabricated and tested under simulated sunlight. **Figure 2E** shows a comparison between spin-coated and spray-coated glass/ITO/CdTe/Ca/Al Schottky devices, where the CdTe nanocrystal layer was solution processed, demonstrating minimal differences between device performance (efficiency = 2.2% for both spin-coated and spray-coated devices).

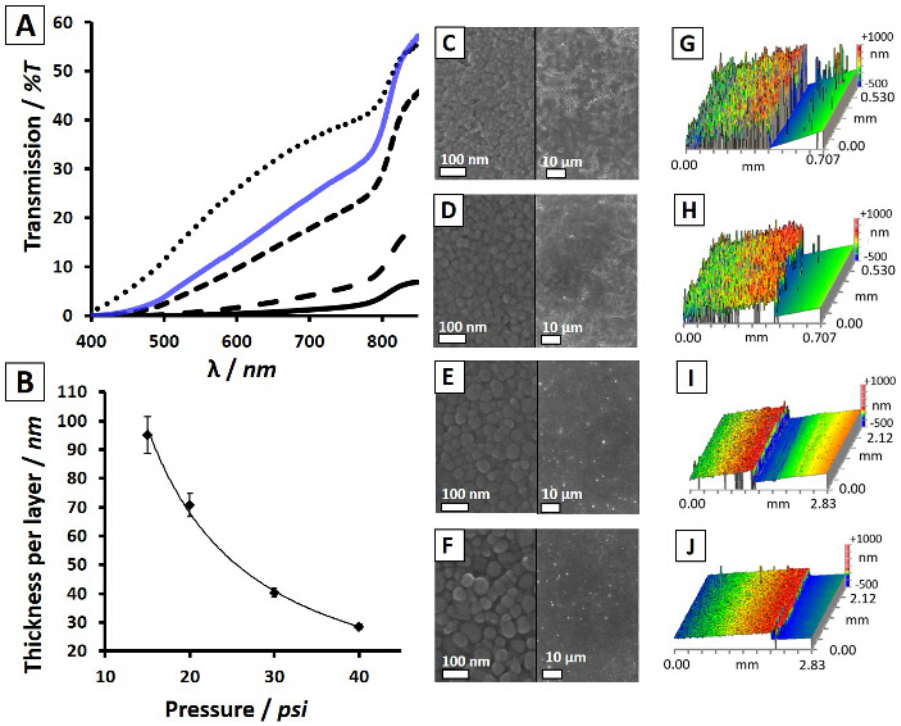

Figure 3. Nanocrystal Spray Pressure and Film Morphology. (**A**) Transmission of light through CdTe device films annealed at 380 °C for 25 s after spray-coated deposition at 15 (—), 20 (- -), 30 (- - -), and 40 psi (⋯) with a spin-coated device (blue—) for comparison. Average film thickness as a function of the spray pressure (**B**). SEM images split with low magnification of CdTe device films spray-coated at 15 (**C**), 20 (**D**), 30 (**E**), and 40 psi (**F**) including corresponding optical profilometry scans showing relative surface roughness (**G**-**J**). Reprinted with permission from Ref. 12. Copyright 2014 American Chemical Society. Please click here to view a larger version of this figure.

Discussion

In summary, this protocol provides guidelines for the key steps involved with building a solution processed electronic device from a spray- or spin-coating deposition. Here, we highlight new methods for solution processing transparent conductive indium tin oxide (ITO) films onto non-conductive glass substrates. After a facile etching procedure, individual electrodes can be formed before spray-depositing the photo-active layers. Using a layer-by-layer technique, CdSe and CdTe nanocrystals can be deposited in air under ambient conditions from an airbrush. After ligand exchange and heat treatment, the final non-transparent conductive metal electrode can be spray-coated onto the device and heated to remove native organic ligands. This layer can also be patterned by using a masking pattern during deposition. The resulting fully solution processed, all-inorganic devices can be characterized and tested.

Particular attention should be directed to using fresh reagents as outdated materials can lead to impure or undesired products. Additionally, the conductivity of the top and bottom electrodes should be tested during device preparation. The ITO film should have a sheet resistance of at least 500 Ohms per square and the top metal film should be at least 20 Ohms per square. If the sheet resistance is higher, apply more layers of this electrode. This becomes particularly important if devices are to be connected in series or parallel as each device needs to be inter-connected electronically. Layer thickness and roughness should be carefully controlled by monitoring the effects of changing air pressure and ink

concentration. Profilometry scans of these films can provide valuable feedback on the spray- or spin-coating parameters. Typically, thin rough films (>100 nm root mean squared) can lead to device shorting and inactive devices. In order to avoid shorting, deposit thicker smoother active layers, and never touch the actual device during fabrication or when measuring.

Compared to existing vacuum deposition of single crystalline materials and common lithographic cleanroom fabrication techniques, ink-based deposition of nanocrystals is less expensive and affords more freedoms to deposit on large areas or irregular surfaces. However, the quality of the interfaces between individual nanocrystals is reduced due to the presence of native organic ligands and the inherent multicrystalline nature of the film. This leads to a higher densities of impurities and defects within the film and consequently, higher electron hole recombination rates. This can be mitigated by using ligand exchange and sintering agents (*e.g.*, NH_4Cl) to enhance crystallinity throughout the film; however, this remains a fundamental issue for inorganic nanocrystal devices. Although, for material systems with a large Bohr-exciton radius like lead sulfide, PbS (~ 20 nm), sintering is not required for effective charge transport between nanocrystals. Additionally, the area of single devices is dependent on the thickness and lateral dimensions of the masking pattern. Large area (>1 cm^2) devices are attainable with macroscale masking patterns; however, microscale or nanoscale patterns would be necessary for micro or quantum dimensional electronic devices.

This video protocol describes methods for the fabrication of ink-based thin film photovoltaic devices from a spray/spin coating process. However, due to the ambient air deposition, without the requirements of vacuum or controlled atmosphere, topics covered here could also be modified for ink-jet printing of inorganic devices. The lower cost of ink-based deposition compared to conventional vacuum deposition and solar cell module packaging could also lower the price of solar power by reducing the fabrication and installation costs. Additionally, this method can be applied to other materials systems and architectures, including organic semiconductors. In addition to photovoltaics, the techniques we describe for solution processing of inorganic materials could be used to construct other electronic devices such as light-emitting diodes (LEDs), capacitors and transistors.

Disclosures

The authors have nothing to disclose.

Acknowledgements

The Office of Naval Research (ONR) is gratefully acknowledged for financial support. A portion of this work was conducted while Professor Townsend held a National Research Council (NRC) Postdoctoral Fellowship at the Naval Research Laboratory and is grateful for internal support from St. Mary's College of Maryland.

References

1. Debnath, R., Bakr, O., & Sargent, E. H. Solution-processed colloidal quantum dot photovoltaics: A perspective. *Energy Environ. Sci.* **4**, 4870-4881 (2011).
2. Tang, J., & Sargent, E. H. Infrared Colloidal Quantum Dots for Photovoltaics: Fundamentals and Recent Progress. *Adv. Mater.* **23**, 12-29 (2011).
3. Ning, Z., Dong, H., Zhang, Q., Voznyy, O., & Sargent, E. H. Solar Cells Based on Inks of n-Type Colloidal Quantum Dots. *ACS Nano.* **8**, 10321-10327 (2014).
4. Yoon, W. et al. Enhanced Open-Circuit Voltage of PbS Nanocrystal Quantum Dot Solar Cells. *Sci. Rep.* **3** (2013).
5. Jiaoyan, Z. *et al.* Enhancement of open-circuit voltage and the fill factor in CdTe nanocrystal solar cells by using interface materials. *Nanotechnology* **25**, 365203 (2014).
6. Kramer, I. J. *et al.* Efficient Spray-Coated Colloidal Quantum Dot Solar Cells. *Adv. Mater.* **27**, 116-121 (2015).
7. Shirasaki, Y., Supran, G. J., Bawendi, M. G., & Bulovic, V. Emergence of colloidal quantum-dot light-emitting technologies. *Nat. Photonics.* **7**, 13-23 (2013).
8. Demir, H. V. et al. Quantum dot integrated LEDs using photonic and excitonic color conversion. *Nano Today.* **6**, 632-647 (2011).
9. Yu, G. et al. Solution-Processed Graphene/MnO2 Nanostructured Textiles for High-Performance Electrochemical Capacitors. *Nano Lett.* **11**, 2905-2911 (2011).
10. Ridley, B. A., Nivi, B., & Jacobson, J. M. All-Inorganic Field Effect Transistors Fabricated by Printing. *Science.* **286**, 746-749 (1999).
11. Habas, S. E., Platt, H. A. S., van Hest, M. F. A. M., & Ginley, D. S. Low-Cost Inorganic Solar Cells: From Ink To Printed Device. *Chem. Rev.* **110**, 6571-6594 (2010).
12. Townsend, T. K., Yoon, W., Foos, E. E., & Tischler, J. G. Impact of Nanocrystal Spray Deposition on Inorganic Solar Cells. *ACS Appl. Mater. Interfaces.* **6**, 7902-7909 (2014).
13. Olson, J. D., Rodriguez, Y. W., Yang, L. D., Alers, G. B., & Carter, S. A. CdTe Schottky diodes from colloidal nanocrystals. *Appl. Phys. Lett.* **96**, 242103 (2010).
14. Sun, S., Liu, H., Gao, Y., Qin, D., & Chen, J. Controlled synthesis of CdTe nanocrystals for high performanced Schottky thin film solar cells. *J. Mater. Chem.* **22**, 19207-19212, (2012).
15. Chen, Z. *et al.* Efficient inorganic solar cells from aqueous nanocrystals: the impact of composition on carrier dynamics. *RSC Adv.* **5**, 74263-74269 (2015).
16. Gur, I., Fromer, N. A., Geier, M. L., & Alivisatos, A. P. Air-stable all-inorganic nanocrystal solar cells processed from solution. *Science.* **310**, 462-465 (2005).
17. Ju, T., Yang, L., & Carter, S. Thickness dependence study of inorganic CdTe/CdSe solar cells fabricated from colloidal nanoparticle solutions. *J. Appl. Phys.* **107**, (2010).
18. MacDonald, B. I. et al. Layer-by-Layer Assembly of Sintered CdSexTe1-x Nanocrystal Solar Cells. *ACS Nano.* **6**, 5995-6004, (2012).
19. Crisp, R. W. *et al.* Nanocrystal Grain Growth and Device Architectures for High-Efficiency CdTe Ink-Based Photovoltaics. *ACS Nano* **8**, 9063-9072 (2014).

20. Townsend, T. K. *et al.* Safer salts for CdTe nanocrystal solution processed solar cells: the dual roles of ligand exchange and grain growth. *J. Mater. Chem. A* **3**, 13057-13065 (2015).
21. Jasieniak, J., MacDonald, B. I., Watkins, S. E., & Mulvaney, P. Solution-Processed Sintered Nanocrystal Solar Cells via Layer-by-Layer Assembly. *Nano Lett.* **11**,2856-2864, (2011).
22. Hecht, D. S., Hu, L. B., & Irvin, G. Emerging Transparent Electrodes Based on Thin Films of Carbon Nanotubes, Graphene, and Metallic Nanostructures. *Adv. Mater.* **23**, 1482-1513 (2011).
23. Kim, M. G., Kanatzidis, M. G., Facchetti, A., & Marks, T. J. Low-temperature fabrication of high-performance metal oxide thin-film electronics via combustion processing. *Nat. Mater.* **10**, 382-388 (2011).
24. Townsend, T. K., & Foos, E. E. Fully solution processed all inorganic nanocrystal solar cells. *Phys. Chem. Chem. Phys.* **16**, 16458-16464 (2014).
25. Yu, W. W., & Peng, X. Formation of High-Quality CdS and Other II-VI Semiconductor Nanocrystals in Noncoordinating Solvents: Tunable Reactivity of Monomers. *Angew. Chem.* **114**, 2474-2477 (2002).
26. Brust, M., Walker, M., Bethell, D., Schiffrin, D. J., & Whyman, R. Synthesis of thiol-derivatised gold nanoparticles in a two-phase Liquid-Liquid system. *J. Chem. Soc., Chem. Commun.* **0**, 801-802 (1994).
27. Smits, F. M. Measurement of Sheet Resistivities with the Four-Point Probe. *Bell Sys. Tech. J.* **37**, 711-718 (1958).
28. Yoon, W., Townsend, T. K., Lumb, M. P., Tischler, J. G., & Foos, E. E. Sintered CdTe Nanocrystal Thin-films: Determination of Optical Constants and Application in Novel Inverted Heterojunction Solar Cells. *IEEE Trans. Nanotechnol.* **13**, 551-556 (2014).
29. Foos, E. E., Yoon, W., Lumb, M. P., Tischler, J. G., & Townsend, T. K. Inorganic Photovoltaic Devices Fabricated Using Nanocrystal Spray Deposition. *ACS Appl. Mater. Interfaces.* **5**, 8828-8832 (2013).
30. Nag, A. *et al.* Metal-free Inorganic Ligands for Colloidal Nanocrystals: S2-, HS-, Se2-, HSe-, Te2-, HTe-, TeS32-, OH-, and NH2- as Surface Ligands. *J. Am. Chem. Soc.* **133**, 10612-10620 (2011).
31. Panthani, M. G. *et al.* High Efficiency Solution Processed Sintered CdTe Nanocrystal Solar Cells: The Role of Interfaces. *Nano Lett.* **14**, 670-675 (2014).

